American Mineralogist, Volume 68, pages 307–314, 1983

The stability of amphibole in andesite and basalt at high pressures[1]

J. C. ALLEN

Department of Geology and Geography
Bucknell University
Lewisburg, Pennsylvania 17837

AND A. L. BOETTCHER

Institute of Geophysics and Planetary Physics
and Department of Earth and Space Sciences
University of California, Los Angeles
Los Angeles, California 90024

Abstract

Some of our earlier work (Allen *et al.*, 1975) on the stability of amphiboles in andesite and basalt at high pressures is subject to criticism because of loss of iron from the starting material to the walls of the capsules ($Ag_{50}Pd_{50}$) during the runs of f_{O_2} buffered over the range of stability of magnetite. Analyses of fused run products show substantial loss of iron from runs at magnetite–wüstite and nickel–nickel oxide conditions, but none from those at magnetite–hematite conditions.

We have now redone our earlier work on the Mt. Hood andesite and 1921 Kilauea olivine tholeiite under N–NO conditions and with silver capsules. Analyses of fused run products show no iron loss, and the reversed curve representing the maximum stability of the amphiboles in the Mt. Hood andesite shows no change in location, although we now have better control on the high-pressure part of this curve. The revised curve for the appearance of garnet is significantly lower in pressure, passing through 15.5 kbar/940°C and 14.5 kbar/900°C. No orthopyroxene appeared in the run products, in contrast to the results of our earlier work. The high-temperature segment of the amphibole-out curve for the tholeiite is at least as high as 1040°C at 13 kbar and 1050°C at 16 kbar, and the high-pressure part of this curve is at about 27 kbars, about 6 kbar higher than in our earlier work. Amphibole is the sole silicate phase on the vapor-saturated liquidus in the andesite at pressures below the garnet-in curve (<15.5 kbar), and it is accompanied by a minor amount of an Fe-rich oxide. The revised phase relationships are consistent with the derivation of andesite by amphibole–liquid equilibria in basaltic magma, and they reveal that the amphiboles are stable to depths of nearly 100 km. The great depths to which amphiboles are stable make it all the more probable that they are a source of H_2O for partial melting in deeply subducted oceanic crust.

Introduction

To understand the role of amphiboles in the genesis of andesites, *e.g.*, by the fractionation of amphiboles from hydrous basaltic magmas in orogenic zones, we (Allen *et al.*, 1975) experimentally established the stabilities of amphiboles in a Mt. Hood andesite, a 1921 Kilauea olivine tholeiite, two other basalts, and an olivine nephelinite in the presence of nearly pure H_2O vapor at values of oxygen fugacity (f_{O_2}) approximately those of Fe_3O_4–Fe_2O_3 (M–H), Ni–NiO (N–NO), and Fe_3O_4–FeO (M–W) from 10 to 36 kbar. Later, we (Allen and Boettcher, 1978) extended that investigation to lower and more realistic values of f_{H_2O} by using H_2O–CO_2 vapors and made all runs at an f_{O_2} approximately that of M–H. Our earlier work (1975), conducted in the presence of nearly pure H_2O vapor, was subject to criticism (Stern and Wyllie, 1975) because of probable loss of iron from the starting material to the walls of the capsules ($Ag_{50}Pd_{50}$). As a result, we determined the amount of iron lost in our earlier experiments by analyzing the glass (quenched liquid) with an electron microprobe analyzer. The results indicated almost total loss of iron from those experiments

---

[1] Institute of Geophysics and Planetary Physics Contribution No. 2297.

0003–004X/83/0304–0307$02.00

Table 1. Experimental run data

P, kbar	T, °C	Run number †	Duration hours	Phase assemblage*
		Andesite		
10	940	A 609	3.0	L,Am,Op,QM
10	960	A 614	3.1	L,Op,QM
13	940	A 561	5.5	L,Am,Op,QM
13	960	A 564	5.5	L,QM
13	980	A 563	5.5	L,QM
14	900	A 611	24.0	L,Am,Op,QM
15	900	A 608	24.2	L,Am,Ga,Op,Ru,QM
15	940	A 593	24.0	L,Am,Op,QM
16	900	A 607	24.0	L,Am,Ga,Op,Ru,QM
16	940	A 565	5.5	L,Am,Ga,Op,QM
17	940	A 567	5.5	L,Am,Ga,Op,QM
17	960	A 603	3.0	L,Op,QM
18	900	A 622	100.0	L,Am,Ga,Cpx,Op,Ru,QM
18	940	A 601	24.0	L,Am,Ga,Op,QM
19	900	A 621	99.0	L,Ga,Cpx,Op,Ru,QM
19	940	A 598	24.0	L,Ga,Op,QM
20	940	A 596	24.0	L,Ga,Op,QM
20	980	A 32	24.0	L,Ga,QM
20	1000	A 33	24.0	L,QM
23	900	A 617	24.0	L,V,Ga,Ru,Op,QM
23	1020	A 28	8.0	L,Ga,QM
23	1040	A 29	8.0	L,QM
25	1040	A 30	8.0	L,Ga,QM
25	1060	A 31	8.0	L,Ga,QM
25	1070	A 34	8.0	L,QM
		**Reversals		
13	965	A 600	6.3	(see run #A 564)
13	935		16.6	L,Am,Op,QM
15.5	900	A 612	24.0	(see run #A 608)
13.5	900		24.5	L,Am,Op,(Ga),QM
20	940	A 623	24.0	(see run #A 596)
17.5	900		100.0	L,Am,Ga,Cpx,Op,QM
		Basalt		
13	1020	B 566	5.5	L,Cpx,Am,Op,QM
13	1030	B 572	5.5	L,Cpx,Am,Op,QM
16	1040	B 577	5.5	L,Cpx,Am,Op,QM
22	1040	B 595	24.0	L,Cpx,Am,Op,QM
23	1040	B 597	24.0	L,Cpx,Am,Ga,Op,QM
23	1070	B 619	23.5	L,Cpx,Am,Ga,Op,QM
25	1040	B 602	24.0	L,Cpx,Am,Ga,Op,QM
26	1020	B 2015	24.0	L,Cpx,Am,Ga,Ru,Op,QM
27	1045	B 2016	24.0	L,Cpx,Ga,Op,QM
28	1020	B 1194	24.0	L,Cpx,Ga,Op,Ru,QM
28	1060	B 1190	24.0	L,Cpx,Ga,Op,QM
		**Reversals		
29	1020	B 2034	20.0	(see run #B 1194)
26	1020		24.0	L,Cpx,Am,Ga,Op,QM

Abbreviations: Am = amphibole; Cpx = clinopyroxene; Ga = garnet; L = glass interpreted to be quenched liquid; M = micaceous mineral; Op = opaque mineral; Ru = rutile; Q = interpreted to have crystallized during the quench; ( ) = trace amount

* *All assemblages include vapor*

† *Run numbers preceded by A employed andesite as a starting material; those preceded by B used basalt.*

** *See text for description of reversal procedure*

at M–W conditions, significant loss at N–NO conditions, but no observable loss at M–H conditions. Thus, the phase relationships reported in our recent investigation (Allen and Boettcher, 1978) are satisfactory for they were done at a sufficiently high f_{O_2}, *i.e.*, M–H, but that part of our earlier work (1975) done at an f_{O_2} lower than approximately M–H was in need of reinvestigation.

Experimental methods

To prevent loss of iron, we have used silver capsules in our reinvestigation of the stability of amphiboles in a Mt. Hood andesite and a 1921 Kilauea olivine tholeiite, for silver does not absorb iron from starting materials. The experiments were accomplished with excess H_2O and at an f_{O_2} approximately that of N–NO. The same techniques described in our earlier papers (1975 and 1978) were used to analyze the run products. No loss of iron was detected. All experiments used a piston-cylinder apparatus similar to that described by Allen *et al.* (1975) and the same furnace assembly and starting materials described by Allen and Boettcher (1978). To reverse the amphibole-out curves, two-stage runs were made in which temperatures were initially held above and then lowered into the stability field of amphibole, as tabulated in Table 1. The phases were identified by the techniques described by Allen *et al.* (1975, p. 1072).

Results

Phase relationships

The phase relationships for the Mt. Hood andesite are given in Table 1 and in Figure 1. A comparison of these

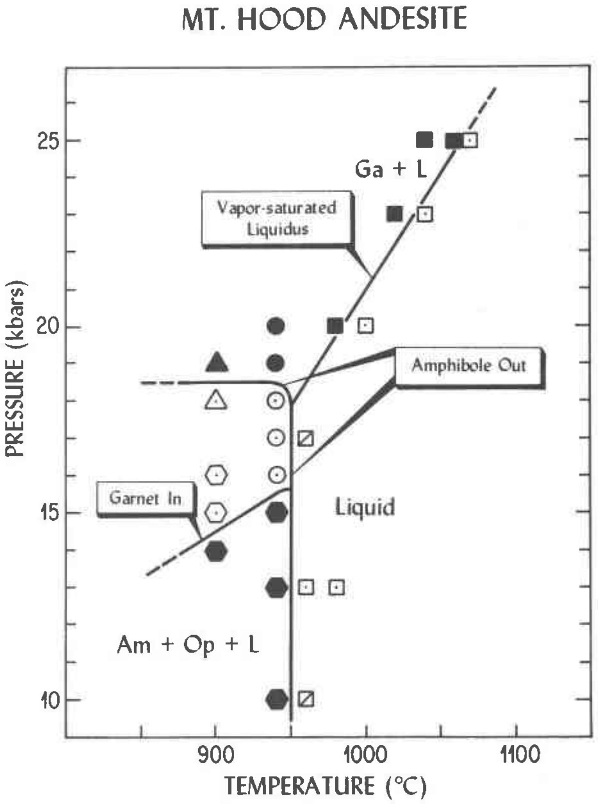

Fig. 1. Crystallization sequence for Mt. Hood andesite. All assemblages coexist with vapor. Abbreviations: Am = amphibole; Ga = garnet; Op = opaque mineral; Cpx = clinopyroxene; Ru = rutile; L = liquid. ⊡ Above liquidus; ⧄ Op + L; ■ Ga + L; ⬢ Am + Op + L; ⊙ Am + Ga + Op + L. ● Ga + Op + L; ⬡ Am + Ga + Op + Ru + L; △ Am + Ga + Op +Cpx + Ru + L; ▲ Ga + Op + Cpx + Ru + L.

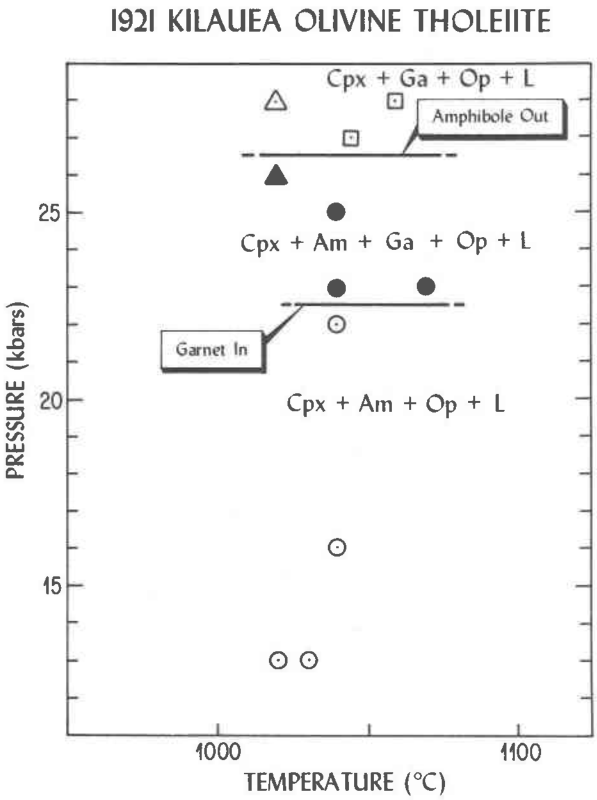

Fig. 2. Crystallization sequence for 1921 Kilauea olivine tholeiite. All assemblages coexist with vapor. Abbreviations: Am = amphibole; Ga = garnet; Op = opaque mineral; Cpx = clinopyroxene; Ru = rutile; L = liquid. ⊙ Cpx + Am + Op + L; ● Cpx + Am + Ga + Op + L; ⊡ Cpx + Ga + Op + L; ▲ Cpx + Am + Ga + Op + Ru + L; △ Cpx + Ga + Op + Ru + L.

relationships determined with Ag capsules with those using $Ag_{50}Pd_{50}$ capsules (Allen *et al.*, 1975) shows no change in the reversed curve representing the stability of amphibole in the andesite, and we now have better control on the relatively flat slope, dP/dT, of the high-pressure part of this curve. However, the garnet-in curve is 2 to 3 kbar lower in the present study. These results are not unexpected, for the amphibole-out curve represents the maximum stability of the amphibole with the highest Mg/(Mg + Fe). Amphiboles with a lower Mg/(Mg + Fe) would melt at lower temperatures, but this would have no significant effect on the location of the high-temperature part of the amphibole-out curve. Similarly, amphibole-bearing assemblages with amphiboles that have a lower Mg/(Mg + Fe) would transform to garnet-bearing assemblages at lower pressures, thereby shifting the garnet-in curve to lower pressures, but this would have no significant effect on the high-pressure part of the amphibole-out curve, at least not in this relatively simple part of the system with few crystalline phases. No orthopyroxene was found in this study with Ag capsules, in contrast to our earlier work.

The phase relationships determined in our reinvestigation of the 1921 Kilauea olivine tholeiite are given in Table 1 and in Figure 2. The melting of silver prevented a complete determination of the melting relationships in this system; however, the high-temperature part of the amphibole-out curve for the tholeiite is at least as high as 1040°C at 13 kbar and 1050°C at 16 kbar. The actual location of this part of the amphibole-out curve is probably not significantly higher, if at all, than the position determined in our earlier study using $Ag_{50}Pd_{50}$ capsules, for, in that study, there was only a small amount of amphibole in the products from the runs at 1030°C and 13 kbar, and at 1040°C and 16 kbar. The high-pressure part of the amphibole-out curve probably has a relatively flat dP/dT slope; amphibole-bearing assemblages start converting to garnet-bearing assemblages at a pressure of about 6 kbar higher than in our earlier study. The garnet-in curve is also substantially higher (2 to 3 kbar) in this study compared to our earlier one. The differences in the location of these two curves compared to those in our earlier work (1975) are not the same or as simple as in the case of the andesite, for there are more complex, crystalline phases in a very complex silicate liquid in the tholeiite compared to the andesite.

Chemical analyses

The chemical composition of clinopyroxenes, amphiboles, garnets and glasses were determined with an ARL–EMX electron microprobe analyzer at UCLA in order to (1) compare the compositions of these phases synthesized in runs with no detectable loss of iron with those in our earlier works (1975, 1978), and (2) determine the potential of amphibole fractionation in these systems at high pressures and high temperatures. The method of Bence and Albee (1968) was used to compute the chemical analyses. The structural formulae of the amphiboles were computed assuming $Fe_2O_3/FeO = 0.4$ to maintain consistency with our earlier methodology. To use the classification of Leake (1978), H_2O in the amphiboles was arbitrarily taken as 2.00 percent, and the structural formulae were calculated using 24 oxygens; however, the structural formulae in Table 3 were computed using 23 oxygens and no H_2O. Salient features of these analyses are as follows:

Clinopyroxene. A direct comparison of these data with those in our earlier paper (Allen *et al.*, 1975) is not possible, for the clinopyroxene in the two investigations were not all synthesized at precisely the same pressures and temperatures; however, those conditions appear to be close enough for a general comparison (this limitation similarly applies to the amphiboles, garnets, and glasses). Our current results (Table 2) are generally consistent with our 1975 data, and they show little variation with changes in pressure and temperature.

Table 2. Clinopyroxene compositions from basalt runs

Analysis	1	2	3	4	5	6	7	8	9
Run #	B 577	B 577	B 595	B 595	B 595	B 597	B 597	B 602	B 602
P,kbar	16	16	22	22	22	23	23	25	25
T,°C	1040	1040	1040	1040	1040	1040	1040	1040	1040
SiO_2	50.83	51.96	51.88	52.31	53.23	53.60	52.02	52.69	51.70
TiO_2	1.15	0.73	0.63	0.64	0.59	0.56	0.59	0.44	0.60
Al_2O_3	4.34	3.52	3.32	2.74	2.40	2.28	3.53	2.07	3.44
FeO*	7.10	6.99	6.58	6.79	6.77	7.44	6.91	7.00	6.69
MgO	15.66	15.49	15.67	15.63	15.37	16.00	16.42	15.99	15.23
MnO	0.17	0.16	0.14	0.12	0.15	0.14	0.15	0.14	0.10
CaO	19.82	20.56	20.97	20.80	20.72	20.58	21.25	20.80	21.69
Na_2O	0.34	0.34	0.49	0.45	0.47	0.43	0.48	0.42	0.52
K_2O	0.05	0.11	0.08	0.06	0.11	0.09	0.12	0.09	0.09
Total	99.45	99.86	99.77	99.53	99.81	101.11	100.49	99.65	100.06
Cations/6 Oxygens									
Si	1.879	1.915	1.908	1.932	1.959	1.951	1.902	1.943	1.898
Al	0.189	0.153	0.144	0.119	0.104	0.098	0.152	0.090	0.149
Ti	0.032	0.020	0.018	0.018	0.016	0.015	0.016	0.012	0.016
Fe	0.220	0.215	0.202	0.210	0.208	0.226	0.211	0.216	0.205
Mg	0.863	0.851	0.859	0.860	0.843	0.868	0.840	0.879	0.833
Mn	0.005	0.005	0.004	0.004	0.005	0.004	0.004	0.004	0.003
Ca	0.785	0.812	0.826	0.823	0.817	0.803	0.833	0.822	0.853
Na	0.024	0.024	0.035	0.032	0.034	0.031	0.034	0.030	0.037
K	0.002	0.005	0.004	0.003	0.005	0.004	0.006	0.004	0.004
$Mg/(Mg+\Sigma Fe)$	0.80	0.80	0.81	0.80	0.80	0.79	0.80	0.80	0.80
Mg	46.2	45.3	45.5	45.4	45.1	45.8	44.6	45.9	44.1
Fe	11.8	11.4	10.7	11.1	11.1	11.9	11.2	11.3	10.8
Ca	42.0	43.2	43.5	43.5	43.7	42.3	44.2	42.9	45.1

* *Total iron as FeO*

Table 3a. Amphibole compositions and structural formulae

Analysis	1	2	3	4	5	6	7	8
Run #	A 611	A 611	A 611	A 608	A 608	A 593	A 593	A 593
P,kbar	14	14	14	15	15	15	15	15
T,°C	900	900	900	900	900	940	940	940
SiO_2	43.58	43.23	44.36	43.51	43.35	43.84	43.95	43.71
TiO_2	1.65	1.97	1.82	1.75	1.65	1.69	1.76	1.72
Al_2O_3	14.86	14.26	13.81	14.15	14.23	13.40	13.47	13.20
Fe_2O_3*	3.89	3.68	3.80	3.84	3.79	3.27	3.27	3.16
FeO	9.74	9.21	9.51	9.60	9.49	8.16	8.17	7.90
MgO	12.66	12.70	12.93	12.46	12.61	14.22	14.54	14.80
MnO	0.18	0.14	0.18	0.17	0.19	0.15	0.15	0.15
CaO	10.30	10.52	10.22	10.43	10.05	10.15	10.25	10.36
Na_2O	2.69	2.67	2.67	2.60	2.63	2.63	2.67	2.72
K_2O	0.50	0.50	0.45	0.48	0.55	0.52	0.54	0.49
H_2O*	2.00	2.00	2.00	2.00	2.00	2.00	2.00	2.00
Total	102.05	100.88	101.75	100.99	100.54	100.03	100.77	100.21
Cations/23 Oxygens								
Si	6.209	6.225	6.323	6.264	6.264	6.322	6.294	6.293
Al^{IV}	1.791	1.775	1.677	1.736	1.736	1.678	1.706	1.707
Al^{VI}	0.704	0.646	0.643	0.666	0.687	0.599	0.568	0.533
Ti	0.177	0.213	0.195	0.189	0.179	0.183	0.190	0.186
Fe^{3+}	0.417	0.399	0.408	0.416	0.412	0.355	0.352	0.342
Mg	2.688	2.726	2.747	2.674	2.716	3.056	3.104	3.176
Fe^{2+}	1.161	1.109	1.134	1.156	1.147	0.984	0.979	0.951
Mn	0.022	0.017	0.022	0.021	0.023	0.018	0.018	0.018
Ca	1.572	1.623	1.561	1.609	1.556	1.568	1.573	1.598
Na	0.743	0.745	0.738	0.726	0.737	0.735	0.741	0.759
K	0.091	0.092	0.082	0.088	0.101	0.096	0.099	0.090
$Mg/(Mg+\Sigma Fe)$	0.63	0.64	0.64	0.63	0.64	0.70	0.70	0.71
$Mg/(Mg+Fe^{2+})$	0.70	0.71	0.71	0.70	0.70	0.76	0.76	0.77
Fe/Mg	0.59	0.55	0.56	0.59	0.57	0.44	0.43	0.41
Classification**	parg	parg	pa-hb	pa-hb	pa-hb	pa-hb	pa-hb	pa-hb

Table 3a. (continued)

Analysis	9	10	11	12	13	14	15	16
Run #	A 607	A 607	A 607	B 595	B 595	B 597	B 602	B 602
P,kbar	16	16	16	22	22	23	25	25
T,°C	900	900	900	1040	1040	1040	1040	1040
SiO_2	43.28	44.07	43.52	40.18	40.66	41.02	42.08	41.65
TiO_2	1.64	1.59	1.76	4.23	3.59	4.02	4.23	3.76
Al_2O_3	15.28	13.62	14.47	12.19	13.81	14.21	13.59	13.25
Fe_2O_3*	3.73	3.89	3.64	3.37	4.10	4.77	4.36	4.08
FeO	9.34	9.74	9.10	8.44	10.24	11.94	10.89	10.21
MgO	12.55	12.94	12.36	12.38	13.45	9.83	9.91	11.21
MnO	0.21	0.22	0.14	0.20	0.21	0.19	0.15	0.17
CaO	10.18	9.49	10.39	12.17	9.16	9.19	9.84	9.83
Na_2O	2.81	2.66	2.65	2.57	2.38	2.29	2.35	2.50
K_2O	0.52	0.40	0.48	0.74	0.67	0.75	0.73	0.76
H_2O*	2.00	2.00	2.00	2.00	2.00	2.00	2.00	2.00
Total	101.54	100.62	100.51	98.47	100.27	100.21	100.13	99.42
Cations/23 Oxygens								
Si	6.186	6.350	6.274	6.010	5.953	6.050	6.174	6.148
Al^{IV}	1.814	1.650	1.726	1.990	2.047	1.950	1.826	1.852
Al^{VI}	0.761	0.663	0.733	0.159	0.336	0.521	0.524	0.453
Ti	0.176	0.172	0.191	0.476	0.395	0.446	0.467	0.417
Fe^{3+}	0.401	0.422	0.395	0.379	0.452	0.529	0.481	0.453
Mg	2.674	2.779	2.656	2.760	2.935	2.161	2.167	2.466
Fe^{2+}	1.116	1.174	1.097	1.056	1.254	1.473	1.336	1.260
Mn	0.025	0.027	0.017	0.025	0.026	0.024	0.019	0.021
Ca	1.559	1.465	1.605	1.950	1.437	1.452	1.547	1.555
Na	0.779	0.743	0.741	0.745	0.676	0.655	0.668	0.715
K	0.095	0.074	0.088	0.141	0.125	0.141	0.137	0.143
$Mg/(Mg+\Sigma Fe)$	0.64	0.64	0.64	0.66	0.63	0.52	0.54	0.59
$Mg/(Mg+Fe^{2+})$	0.71	0.70	0.71	0.72	0.70	0.59	0.62	0.66
Fe/Mg	0.57	0.57	0.56	0.52	0.58	0.93	0.84	0.69
Classification**	parg	pa-hb	pa-hb	mg-ha	mg-ha	ts	ts	ts

* *Estimate, see text.*

** *On the basis of 24 oxygens, according to classification of Leake (1978)*
Abbreviations: parg = pargasite; pa-hb = pargasitic hornblende; mg-ha = magnesio-hastingsite; ts = tschermakite; A = Andesite; B = Basalt
Analyses 1-11 from andesite; analyses 12-16 from basalt.

Amphiboles. Our 1975 data for amphiboles synthesized from the andesite were significantly higher in SiO_2 and somewhat higher in MgO, about the same in Fe_2O_3 and FeO, and significantly lower in Al_2O_3 at lower pressures, but somewhat higher in FeO and Fe_2O_3 and lower in MgO and CaO at higher pressure. Our present results (Table 3) show a decrease in FeO and Fe_2O_3 and an increase in MgO with an increase in temperature at a constant pressure, but they show no significant change with variations in pressure. Our 1975 data for amphiboles synthesized from the basalt were highly variable and significantly lower in TiO_2 and higher in Al_2O_3.

Garnets. Garnets synthesized from the andesite are significantly lower in SiO_2 and higher in Al_2O_3 and FeO* than in our 1975 study. The garnets in Table 4 show a decrease in FeO* and an increase in MgO with an increase in temperature at constant pressure.

Glasses. The variation in sodium among these rather H_2O–rich glasses (Table 5) is most likely to have been the result of the volatilization of sodium. These analyses are reported on an anhydrous basis; the totals before recalculation on this basis ranged from 74.98 to 91.80%. Although the glasses were generally clear and free of quench crystals, it is possible that minute grains, for instance of opaque minerals, may be responsible for some of the compositional variation. The glasses (Table 5) formed from the andesite are richer in FeO, Fe_2O_3, MgO, and Na_2O than those in our 1975 study, but Mg/(Mg + ΣFe) is similar. Note that the glasses formed from the basalt are significantly higher in SiO_2, Al_2O_3, and K_2O, and lower in the other major oxides than the parent basalt. All of the glasses in Table 5 are quartz-normative.

Discussion

The results of our reinvestigation indicate that there is no need to significantly alter the conclusions or applica-

Table 3b. Normative composition (C.I.P.W.) of amphiboles in Table 3a

Norm	1	2	3	4	5	6	7	8
orthoclase	2.96	2.96	2.66	2.84	3.25	3.07	3.19	2.90
albite	10.36	9.91	13.34	11.17	11.21	11.15	10.24	9.47
anorthite	27.00	25.45	24.37	25.52	25.40	23.22	23.18	22.36
nepheline	6.72	6.87	5.01	5.87	5.98	6.02	6.69	7.34
diopside	19.38	21.45	21.14	21.09	19.66	21.65	22.08	23.14
wo	(10.06)	(11.17)	(11.00)	(10.95)	(10.21)	(11.33)	(11.56)	(12.12)
en	(6.71)	(7.65)	(7.45)	(7.33)	(6.85)	(8.09)	(8.30)	(8.79)
fs	(2.61)	(2.63)	(2.70)	(2.81)	(2.60)	(2.23)	(2.22)	(2.23)
olivine	24.86	23.17	24.26	23.62	24.41	24.97	25.32	25.16
fo	(17.39)	(16.80)	(17.34)	(16.61)	(17.21)	(19.15)	(19.56)	(19.67)
fa	(7.47)	(6.37)	(6.92)	(7.01)	(7.20)	(5.82)	(5.76)	(5.49)
magnetite	5.64	5.34	5.51	5.57	5.50	4.74	4.74	4.58
ilmenite	3.13	3.74	3.46	3.32	3.13	3.21	3.34	3.27

Norm	9	10	11	12	13	14	15	16
orthoclase	3.07	2.36	2.84	4.37	3.96	4.43	4.31	4.49
albite	9.77	15.39	11.55	0.17	8.26	13.34	14.60	11.20
anorthite	27.55	24.04	26.17	19.54	25.02	26.28	24.38	22.69
nepheline	7.59	3.86	5.89	11.69	6.44	3.27	2.86	5.40
diopside	18.45	18.52	20.37	32.40	16.33	15.61	19.66	20.91
wo	(9.59)	(9.62)	(10.60)	(17.05)	(8.53)	(8.06)	(10.20)	(10.89)
en	(6.44)	(6.42)	(7.19)	(12.81)	(6.02)	(5.11)	(6.79)	(7.48)
fs	(2.42)	(2.48)	(2.58)	(2.54)	(1.78)	(2.44)	(2.67)	(2.54)
olivine	24.60	25.78	23.07	15.38	25.51	20.72	17.96	19.68
fo	(17.39)	(18.08)	(16.53)	(12.63)	(19.25)	(13.57)	(12.54)	(14.32)
fa	(7.21)	(7.70)	(6.54)	(2.75)	(6.26)	(7.15)	(5.42)	(5.36)
magnetite	5.41	5.64	5.28	4.89	5.95	6.92	6.32	5.92
ilmenite	3.12	3.02	3.34	8.03	6.82	7.64	8.03	7.14

Table 4. Garnet compositions

Analysis	1	2	3	4	5	6	7	8	9	10	11
Run #	A 622	A 601	A 621	A 598	A 598	A 615	A 596	A 596	A 616	A 617	B 602
P,kbar	18	18	19	19	19	20	20	20	22	23	25
T,°C	900	940	900	940	940	900	940	940	900	900	1040
SiO_2	40.35	40.06	37.77	39.33	40.04	38.35	38.17	39.26	38.51	38.40	40.16
TiO_2	1.36	1.32	1.99	1.08	1.94	1.98	2.40	1.96	2.32	2.03	1.89
Al_2O_3	20.24	21.82	21.21	22.33	21.29	20.38	20.33	20.64	20.76	21.07	20.38
FeO^*	20.05	19.77	20.74	19.51	19.78	20.95	20.04	19.03	20.52	19.16	15.91
MgO	7.48	9.28	7.04	9.43	9.35	7.04	7.77	9.39	5.76	7.31	11.41
MnO	0.75	0.55	0.84	0.52	0.64	0.88	0.85	0.39	0.85	0.53	0.49
CaO	9.85	9.79	10.63	9.56	9.77	10.41	10.15	9.92	12.13	11.36	10.20
Na_2O	0.06	0.06	0.04	0.06	0.06	0.07	0.06	0.07	0.08	0.10	0.04
K_2O	0.15	0.07	0.14	0.04	0.02	0.07	0.14	0.14	0.08	0.12	0.08
Total	100.28	102.73	100.39	101.86	102.89	100.12	99.90	100.78	101.01	100.08	100.57
Cations/ 12 Oxygens											
Si	3.084	2.958	2.892	2.921	2.960	2.950	2.932	2.957	2.947	2.935	2.990
Al	1.824	1.900	1.915	1.956	1.855	1.849	1.841	1.832	1.873	1.899	1.789
Ti	0.078	0.073	0.115	0.060	0.108	0.115	0.139	0.111	0.134	0.117	0.106
Fe	1.282	1.221	1.329	1.212	1.223	1.348	1.287	1.199	1.313	1.225	0.991
Mg	0.853	1.022	0.803	1.044	1.030	0.807	0.889	1.054	0.657	0.833	1.266
Mn	0.049	0.035	0.054	0.033	0.040	0.057	0.055	0.025	0.055	0.034	0.031
Ca	0.807	0.775	0.872	0.761	0.774	0.858	0.835	0.800	0.995	0.930	0.814
Na	0.009	0.009	0.007	0.009	0.009	0.010	0.009	0.010	0.012	0.014	0.006
K	0.015	0.007	0.013	0.004	0.002	0.006	0.014	0.013	0.008	0.012	0.007
Mg/(Mg+ΣFe)	0.40	0.46	0.38	0.46	0.46	0.37	0.41	0.47	0.33	0.40	0.56

* *Total iron as FeO.*
Abbreviations: A = Andesite; B = Basalt
Analyses 1-10 from andesite; analyses 11 from basalt.

Table 5a. Composition of quenched liquids

Analysis	1	2	3	4	5	6	7
Run #	A 608	A 607	A 621	A 621	B 597	B 597	B 602
P,kbar	15	16	19	19	23	23	25
T,°C	900	900	900	900	1040	1040	1040
SiO_2	65.46	65.87	66.80	67.14	67.17	54.08	63.54
TiO_2	0.60	0.57	0.65	0.44	0.34	1.41	1.81
Al_2O_3	17.49	18.45	16.57	17.77	19.67	19.01	19.90
Fe_2O_3*	0.67	1.66	0.86	0.72	1.36	3.11	0.85
FeO	1.66	4.14	2.14	1.80	3.38	7.77	2.12
MgO	1.39	2.33	1.54	1.12	0.66	2.46	1.16
MnO	0.03	0.06	0.00	0.00	0.04	0.26	0.09
CaO	5.41	5.03	4.50	4.38	5.70	9.00	7.46
Na_2O	6.26	1.90	5.87	5.37	0.36	1.45	1.21
K_2O	1.01	0.00	1.10	1.27	1.33	1.44	1.84
Total	99.98	100.01	100.03	100.01	100.01	99.99	99.98
$Mg/(Mg+\Sigma Fe)$	0.37	0.29	0.34	0.31	0.12	0.18	0.28

* *Estimate, see text.*
Analyses 1-4 from andesite; analyses 5-7 from basalt.

tions discussed in our previous papers (Allen *et al.*, 1975; Allen and Boettcher, 1978). Our current study confirms that the stability of amphiboles in andesites and basalts is limited by melting reactions at high temperatures and by transformation to garnet-bearing assemblages at high pressures. Amphiboles in the basalt are stable to temperatures greater than those of the vapor-saturated liquidus for the andesite. The separation of low-silica amphiboles (such as those synthesized from the tholeiite in this study) from basaltic magmas by partial melting or fractional crystallization in the presence of water would be an effective process leading toward silica enrichment of the liquid, such as proposed by Bowen (1928) and applied to derivation of andesitic magmas by Boettcher (1977). Nevertheless, recent investigations of orogenic-zone andesites (*e.g.*, Gill, 1981) reveal that the genesis of such rocks is far too complex to be modeled by such processes alone.

The most important revelation of this work is that the maximum depth to which amphiboles are stable in basaltic compositions is almost 100 km, which is significantly greater than that suggested by our earlier work. These great depths to which amphiboles are stable enhance the likelihood that they are a source of H_2O for partial melting in deeply subducted oceanic crust.

Acknowledgments

This research was supported by NSF Grant EAR78-16413 to ALB. Dr. M. J. Rutherford reviewed the manuscript. Robert Jones provided able guidance on the microprobe analyzer. We thank Harriett Arnoff for typing the manuscript and Victoria Jones for her drafting.

Table 5b. Normative composition (C.I.P.W.) of liquids in Table 5a

Norm	1	2	3	4	5	6	7
quartz	13.01	38.11	16.98	19.32	44.69	13.46	31.58
orthoclase	5.97	0.00	6.50	7.51	7.86	8.51	10.87
albite	52.97	16.08	49.67	45.44	3.05	12.27	10.24
anorthite	16.64	24.95	15.62	20.63	28.28	41.11	37.01
corundum	0.00	6.18	0.00	0.00	7.28	0.00	2.36
diopside	8.10	0.00	5.45	0.90	0.00	2.80	0.00
wo	(4.20)	0.00	(2.80)	(0.46)	0.00	(1.40)	0.00
en	(2.70)	0.00	(1.70)	(0.26)	0.00	(0.50)	0.00
fs	(1.20)	0.00	(0.95)	(0.18)	0.00	(0.90)	0.00
hypersthene	1.00	11.20	3.34	4.33	6.10	14.40	3.26
en	(0.70)	(5.80)	(2.14)	(2.53)	(1.60)	(5.50)	(2.89)
fs	(0.30)	(5.40)	(1.20)	(1.80)	(4.50)	(8.90)	(0.37)
magnetite	0.97	2.41	1.25	1.04	1.97	4.51	1.23
ilmenite	1.14	1.08	1.24	0.84	0.65	2.68	3.44

References

Allen, J. C. and Boettcher, A. L. (1978) Amphiboles in andesite and basalt: II. Stability as a function of P–T–f_{H_2O}–f_{O_2}. American Mineralogist, 63, 1074–1087.

Allen, J. C., Boettcher, A. L., and Marland, G. (1975) Amphiboles in andesite and basalt: I. Stability as a function of P–T–f_{O_2}. American Mineralogist, 60, 1069–1085.

Bence, A. E. and Albee, A. L. (1968) Empirical correction factors for the electron-microanalysis of silicates and oxides. Journal of Geology, 76, 382–403.

Boettcher, A. L. (1977) The role of amphiboles and water in circum-Pacific volcanism. In M. H. Manghnani and S. Akimoto, Eds., High-Pressure Research, Applications in Geophysics, p. 107–125. Academic Press, London.

Bowen, N. L. (1928) The Evolution of the Igneous Rocks. Princeton University Press, Princeton.

Gill, J. B. (1981) Orogenic Andesites and Plate Tectonics. Springer-Verlag, New York.

Leake, B. E. (1978) Nomenclature of amphiboles. Canadian Mineralogist, 16, 501–520.

Stern, C. R. and Wyllie, P. J. (1975) Effect of iron absorption by noble-metal capsules on phase boundaries in rock-melting experiments at 30 kilobars. American Mineralogist, 60, 681–689.

Manuscript received, March 30, 1982;
accepted for publication, October 8, 1982.